

# Incorporation of Dyes into Polystyrene-*block*-poly(4-vinylpyridine) Nanotemplates

Radim Křenek,<sup>\*1</sup> Věra Cimrová,<sup>2</sup> Manfred Stamm<sup>1</sup>

**Summary:** The present study provides some basic concepts of functionalization of diblock copolymer (BC) nanotemplates for optical applications. It is focused on the polystyrene-*block*-poly(4-vinylpyridine) (PS-*b*-P4VP) building medium which is suitable for hydrogen bonding, undergoes phase segregation, and is well-accessible. Two techniques are described and demonstrated on several dye complexes with PS-*b*-P4VP. Relation between optical properties and thin film structure is tentatively studied in dependence on solvent effects in thin films.

**Keywords:** diblock copolymers; dyes/pigments; functionalization of polymers; templates

## Introduction

Thin films with ordered nanoarrays of active elements (luminescent, photochromic, photoconductive) are promising for many optoelectronic applications. The group of Ikkala first studied complexes of PS-*b*-P4VP diblock copolymers with low-molar-weight additives (LMA) in the bulk.<sup>[1]</sup> Co-existence of spherical and cylindrical microdomains was observed upon equimolar blending of 3-pentadecylphenol to the monomer units (4VP) of P4VP block by Tokarev.<sup>[2]</sup> Sidorenko et al. succeeded in preparation of a supramolecular assembly with PS-*b*-P4VP, using azobenzene with two hydrogen bond donors: 2-[(4-hydroxybenzene)azo]benzoic acid (*ortho*-HABA).<sup>[3]</sup> Such assembly provided cylindrical morphology throughout the whole film in normal direction to the substrate, except a 2 nm thin adhesion layer.<sup>[4]</sup> Moreover, lateral order and orientation can be controlled via vapor annealing

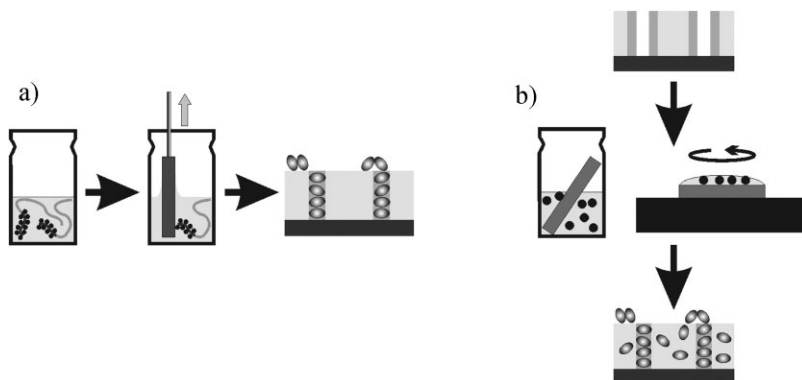
and *ortho*-HABA can be rinsed with a selective solvent.<sup>[4]</sup> *Ortho*-HABA is in this case blocked for photochromism, but it is suitable as a temporary filler for development of ordered porous nanotemplates. UV-Vis spectrophotometry proved that *ortho*-HABA is completely removed already after 2 min rinsing in methanol.<sup>[3]</sup> In this paper, we deal with two approaches of PS-*b*-P4VP functionalization: 1) direct blending of BC with LMA and 2) loading of LMA into porous nanotemplates developed by self-assembling PS-*b*-P4VP and *ortho*-HABA via soaking or spin-coating (see Figure 1).

## Direct Functionalization

The concept of direct functionalization (Figure 1a) is based on modification of a diblock copolymer in solution with LMA and subsequent thin film deposition. A functional additive is dissolved together with PS-*b*-P4VP and relaxed in order to form hydrogen bonds, and subsequently the film is prepared by dip- or spin-coating on an appropriate substrate. In this study we used PS-*b*-P4VP ( $M_{n,PS} = 34\,000$ ,  $M_{n,P4VP} = 2\,900$ ,  $M_{w,BC}/M_{n,BC} = 1.07$ , Polymer Source Inc.) with a luminescent additive, 1-pyrenemethanol, PyM, (Aldrich). Although PyM is well soluble in many solvents,

<sup>1</sup> Department of Nanostructured Materials, Leibniz Institute of Polymer Research Dresden, Hohe Str. 6, D-01069 Dresden, Germany  
E-mail: krenek@ipfdd.de

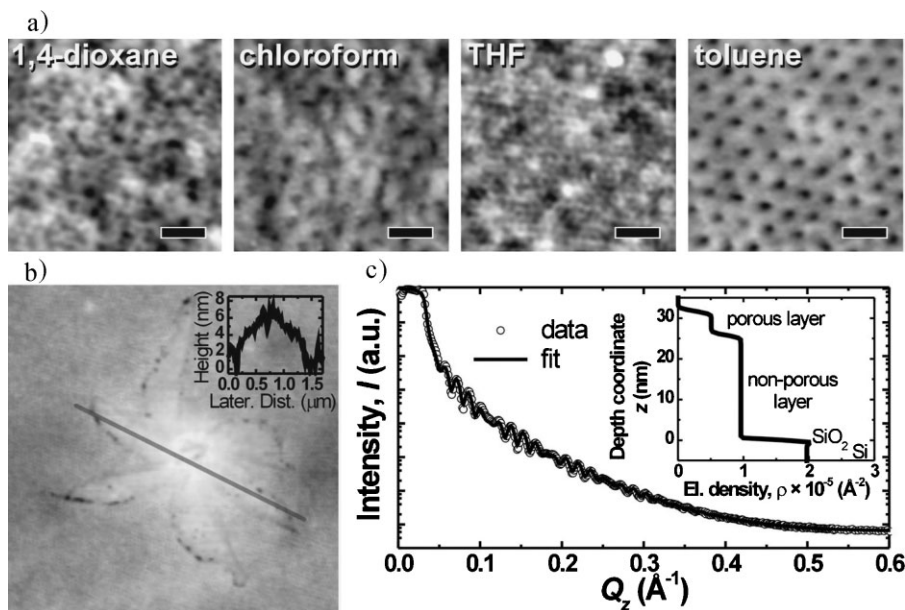
<sup>2</sup> Institute of Macromolecular Chemistry, Academy of Sciences of the Czech Republic, Heyrovsky Sq. 2, 162 06 Prague 6, Czech Republic

**Figure 1.**

Schematic view of (a) direct functionalization and (b) post-functionalization.

ordered film topography was observed only in an equimolar (PyM:4VP) self-assembled film cast from toluene (Figure 2a) onto fused silica slides (*PGO GmbH*, Iserlohn, Germany) for the optical study. Despite of similarity of the topography pattern to that of *ortho*-HABA assembly,<sup>[3]</sup> we observed

rarely distributed aggregates in otherwise smooth films (Figure 2b). A refractive index of 1.58 of the porous PyM-based nanotemplate, measured with a SE400 ellipsometer (*SENTECH Instruments GmbH*, Berlin, Germany),<sup>[4]</sup> results in only 9% of porous layer on the overall thickness of the film. A

**Figure 2.**

(a) AFM topography (50 nm scale bar) of PyM assemblies with PS-*b*-P4VP copolymer cast from various solvents and rinsed with methanol (film thicknesses about 30 nm). (b) AFM topography with a vertical profile (taken along the line and depicted in the inset) of PyM aggregate in the toluene cast assembly prior rinse in methanol. (c) X-ray reflectivity curve with a fit and the calculated electron density profile of the toluene-cast assembly on a Si(100) wafer after PyM rinse with methanol.

vertical electron density profile (the inset in Figure 2c), obtained by fitting the x-ray reflectivity curve (Figure 2c, obtained with a XRD 3003 T/T diffractometer, *Seifert-FPM*, Freiberg, Germany), demonstrates that the porous layer is situated on the top of the film and occupies 19% of the overall thickness.

Absorption and photoluminescence spectra of two thin films of PyM+PS-*b*-P4VP spin-cast from toluene without vapor annealing and after annealing in saturated toluene vapors for 10 min are shown in Figure 3. The PL emission consists of the NUV emission at about 380–400 nm corresponding to pyrene monomer fluorescence and a broad-band emission in the visible region typical of the pyrene excimer with a maximum located at about 470 nm. The PL excimer emission decreased after annealing as the order in the film increased (Figure 3) indicating that reorganization of PyM molecules in microdomains suppresses dimer interactions.<sup>[5]</sup> For comparison, we prepared thin layers made of blends of PyM and carboxy-terminated polystyrene (PSCOOH,  $M_n = 4700$ ,  $M_w/M_n = 1.09$ , *Polymer Source Inc.*) in the same weight ratio as PyM with PS-*b*-P4VP ( $m_{\text{PyM}}/m_{\text{PSCOOH}} = m_{\text{PyM}}/m_{\text{PS-}b\text{-P4VP}}$ ). As expected, due to more random orientation of PyM molecules in the PSCOOH blend than in

the PS-*b*-P4VP blend, a higher contribution of excimer emission in the PL emission was detected.

Further, we used 5(6)-carboxyfluorescein, COF, (*Fluka*) as a low-molecular-weight luminescent additive, which is soluble in polar solvents due to its carboxylic group, but it may be dissolved well in pyridine, too. We studied COF assemblies with PS-*b*-P4VP copolymer and also with P4VP ( $M_n = 5100$ ,  $M_w/M_n = 1.09$ , *Polymer Source Inc.*) for comparison. Thin films were cast from 2% (w/v) pyridine solutions (COF:4VP was 1:3). Thin films made of COF with PS-*b*-P4VP were studied without annealing (**BCn**) and also after annealing in 1,4-dioxane (**BCd**) or chloroform (**BCc**) vapor. Their optical properties (Figure 4) significantly differ from those measured in films made of COF with P4VP. The absorption coefficient of COF+P4VP thin layers is much higher than in COF assembly with PS-*b*-P4VP copolymer (Figure 4a), in which COF is grafted on the minor block of BC (ca. 20% of volume). PL efficiency of the ordered COF+PS-*b*-P4VP assembly is several times higher than that of COF+P4VP (Figure 4b). The dilution effect and also orientation of COF molecules influence the PL emission efficiency. Aggregation effects at the blending ratio (1:3) are assumed to be little important.

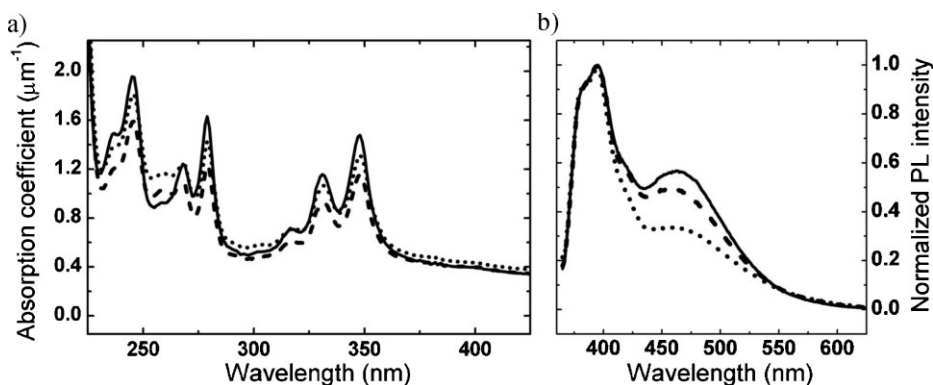


**Figure 3.**

(a) UV-vis absorption and (b) normalized photoluminescent emission of 30-nm films made of: PyM+PSCOOH (solid), PyM+PS-*b*-P4VP (from toluene) without annealing (dash) and after annealing (dot). Excitation wavelength was 345 nm.

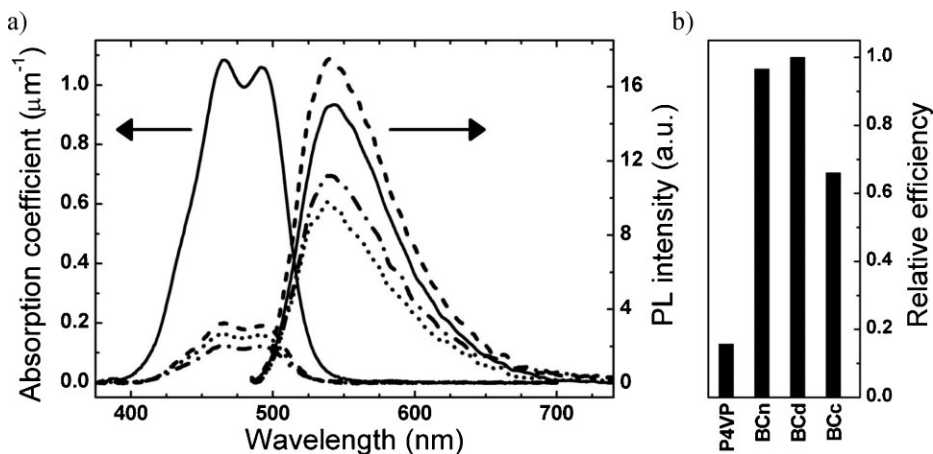


**Figure 4.**

(a) UV-Vis absorption and PL emission, and (b) relative PL efficiency of 50-nm films made of blends: COF + P4VP (solid) and COF + PS-*b*-P4VP: **BCn** without annealing (dash), **BCd** annealed in dioxane (dash-dot) or **BCc** annealed in chloroform (dot) vapor. Excitation wavelength was 465 nm.

### Post-Functionalization

For post-functionalization we used highly ordered porous nanotemplates developed via *ortho*-HABA (2-[(4-hydroxyphenyl) azo]benzoic acid).<sup>[3,4]</sup> Prior to impregnation with a dye, the porous nanotemplate was stabilized by UV irradiation for 30 min.<sup>[6]</sup> As a dye we used Rhodamine 6G (R6G, Merck). The nanotemplate films were soaked in 0.01% (w/v) solutions of R6G in methanol (**Nm**) or in 1,4-dioxane (**Nd**)

for 5 h. The samples were then shortly rinsed in fresh solvent in order to reduce aggregates on the surface and subsequently dried. Absorption and PL spectra of **Nm** and **Nd** are shown in Figure 5.

Absorption spectra showed that soaking in a dioxane solution was much more efficient than that in a methanol solution. R6G molecules can be easily captured by the film in a dioxane solution in comparison with a methanol solution. On the other

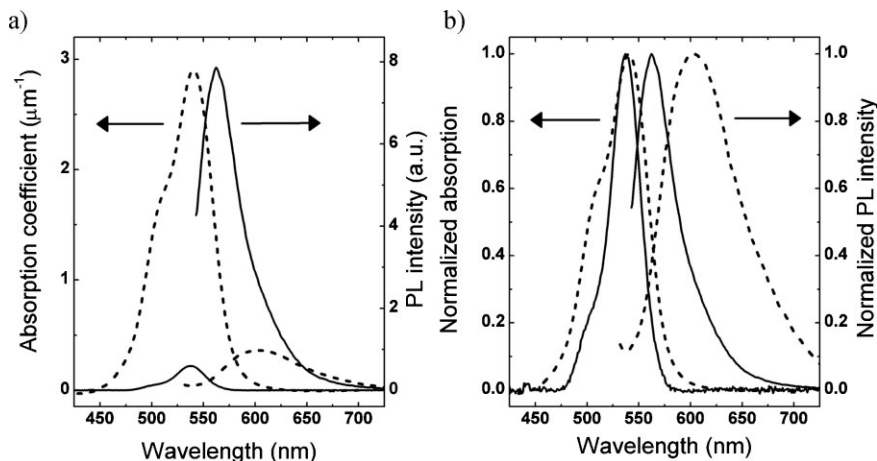


**Figure 5.**

(a) UV-Vis absorption and PL emission, and (b) normalized spectra of 50-nm films prepared via soaking of porous crosslinked nanotemplates in 1,4-dioxane (**Nd**, dash) and methanol (**Nm**, solid) solutions of R6G.

hand, a much higher PL emission intensity was observed for the thin **Nm** films than for the **Nd** films. Compared with the PL emission maximum in **Nm** located at 562 nm, the maximum in **Nd** was red-shifted, located at 603 nm, indicating pronounced dimerization of R6G in **Nd** (Figure 5b). This is also apparent from the absorption spectra where the significant shoulder at 500 nm in **Nd** corresponds to dimers, and the maximum at about 530 nm can be assigned to the monomer.<sup>[7,8]</sup> These results are consistent with the fact that in methanol only monomeric form of R6G is present up to high concentrations and in non-polar solvents R6G molecules form dimeric aggregates.<sup>[8]</sup> It was found that PL emission of R6G in a nanocomposite is dependent on the host matrix and is red-shifted with increasing dye concentration.<sup>[9–11]</sup>

## Conclusion

We presented two approaches for functionalization of PS-*b*-P4VP nanotemplates: direct and post-functionalization. We observed pronounced enhancements in photoluminescent emission in oriented and ordered dyes assemblies with PS-*b*-P4VP in comparison with homopolymer assemblies. We have shown that formation of the assemblies and optical properties are dependent on solvent, which determines

morphology of thin films and interaction of dye molecules.

**Acknowledgements:** We acknowledge the support of the European Network of Excellence Nanofun-Poly, the Grant Agency of the Academy of Sciences of the Czech Republic (grant No. IAA4050409), the Ministry of Education, Youth and Sports of the Czech Republic (grant No.1M06031) and the German Research Foundation (the priority program 1165: Nanowires and Nanotubes).

- [1] R. Mäki-Onto, K. de Moel, W. de Odorico, J. Ruokolainen, M. Stamm, G. ten Brinke, O. Ikkala, *Adv. Mater.* **2001**, 13, 117.
- [2] I. Tokarev, *PhD Thesis*, Sächsische Landes- Staats- und Universitätsbibliothek (SLUB), Dresden **2004**, Chapter 7.
- [3] A. Sidorenko, I. Tokarev, S. Minko, M. Stamm, *J. Am. Chem. Soc.* **2003**, 125, 12211.
- [4] I. Tokarev, R. Krenek, Y. Burkov, D. Schmeisser, A. Sidorenko, S. Minko, M. Stamm, *Macromolecules* **2005**, 38, 507.
- [5] F. M. Winnik, *Chem. Rev.* **1993**, 93, 587.
- [6] Y. Sun, V. Luchnikov, M. Stamm, *Polym. Mater. Sci. Eng.* **2006**, 51, 721.
- [7] F. del Monte, J. D. Mackenzie, D. Levy, *Langmuir* **2000**, 16, 7377.
- [8] P. Innocenzi, H. Kozuka, T. Yoko, *J. Non-Cryst. Solids* **1996**, 201, 26.
- [9] G. Hungerford, K. Suhling, J. A. Ferreira, *J. Photochem. Photobiol., A* **1999**, 129, 71.
- [10] R. Vogel, P. Meredith, M. D. Harvey, H. Rubinsztein-Dunlop, *Spectrochim. Acta, Part A* **2004**, 60, 245.
- [11] S. S. Kurbanov, Z. Sh. Shaymardanov, M. A. Kasymdzhanov, P. K. Khabibullaev, T. W. Kang, *Opt. Mater.* **2007**, 29, 1177.